

PSO-SVM-based deep displacement prediction of Majiagou landslide considering the deformation hysteresis effect

Abstract The accuracy of landslide displacement prediction can effectively prevent casualties and economic losses. To achieve accurate prediction of the Majiagou landslide displacement in the Three Gorges Reservoir (TGR), China, a hybrid machine learning prediction model considering the deformation hysteresis effect is proposed. The real-time deep displacement measurements were captured by using in-place inclinometers with Fiber Bragg grating (FBG) sensors. The time series method was adopted to divide the total displacement into a trend term and periodic term. Trend displacement was determined by the geological condition and predicted by the fitting method. Periodic displacement was controlled by external factors such as rainfall and fluctuation of reservoir water level. Before making the prediction, the grey correlation analysis was adopted to confirm that the fluctuation of the reservoir water level was the main influence factor. In view of the deficiency that current prediction methods could not quantitatively determine the lag time of landslide deformation and thus select the influencing factors empirically, the dynamic analysis of the correlation between periodic influence factors and periodic displacement was carried out in this paper, and the deformation lag time was identified to be 18 days by using set pair analysis (SPA) method. Finally, the optimal influence factors were selected and the prediction model of Majiagou landslide based on support vector machine optimized by particle swarm optimization (SPA-PSO-SVM) was established. Results showed that the root mean square error (RMSE) and the mean absolute percentage error (MAPE) of the proposed SPA-PSO-SVM prediction model are 0.28 and 12.8, respectively. Compared with the PSO-SVM model, the prediction accuracy of the proposed model had been improved significantly. The reliability and effectiveness of the SPA-PSO-SVM prediction model is verified and it has apparent advantages while predicting landslide displacement with deformation hysteresis effect involved.

Keywords Reservoir landslide · Fiber Bragg grating (FBG) · Set pair analysis (SPA) · PSO-SVM · Displacement prediction · Deformation hysteresis effect

Introduction

In the history of reservoir landslides, the 1963 Vajont landslide in Italy is the most famous one. This landslide destroyed a village downstream, resulting in thousands of deaths (Wolter et al. 2014; Carlà et al. 2017). Since the first impoundment of the Three Gorges Reservoir (TGR), Hubei Province, China, in June 2003, more than 5000 landslides have occurred, which poses a great threat to the safety of people's lives and property (Wang and Li 2009). In July 2003, Qianjiangping landslide in this region slid into the Qinggan-he River at a high speed, causing 24 losses and destroying 346 houses (Wang et al. 2004a; Jiao et al. 2014). Long-term

monitoring and early warning of such landslides, therefore, is of great importance and has been paid much attention in the past two decades.

The accuracy of landslide displacement prediction depends on the precision of the prediction model (Huang et al. 2017; Zhang et al. 2019). Since the 1960s, the studies on landslide displacement prediction have experienced three stages: the empirical prediction stage, the statistical prediction stage, and the non-linear prediction stage (Li and Xu 2003). In the non-linear prediction stage, the landslide displacement prediction adopts the method of superposition the total displacement into the trend and periodic term. Among them, trend displacement, usually in the form of steady growth, reflects the main trend of landslide evolution. It is usually predicted by fitting method (Vallet et al. 2016). The periodic displacement fluctuates with the variation of various external factors. Therefore, the appropriate selection of influence factors is critical for the reliable prediction of periodic displacement. Miao et al. (2018) selected the 1- and 2-month precipitation, 1- and 2-month reservoir water level, and annual displacement rate as the influencing factors while predicting the displacement of Baishuihe landslide. Similarly, the monthly rainfall intensity, the monthly average reservoir water level, the monthly variation in the reservoir water level, and the monthly displacement velocity were adopted as the influence factors for Zhujiadian landslide displacement prediction (Ma et al. 2017). It can be found that as the lag time of landslide deformation cannot be accurately identified, the influencing factors are often empirically selected, which will surely lead to errors in prediction results. In view of this, this paper introduces a simple but efficient algorithm named set pair analysis (SPA). By continuously translating the periodic terms of influencing factors and displacement, the maximum of the objective function (the identical degree) can be found. Then the lag time of deformation can be thereby identified. Besides, the quality of field monitoring data is also very important. At present, the global positioning system (GPS) is widely used in landslide deformation monitoring (Akbarimehr et al. 2013; Baldi et al. 2008). However, this method can only obtain the surface displacements, and the measuring accuracy is greatly affected by environmental factors (Sun et al. 2014). In addition, the minimum time interval of monitored data is about 1 month. Given that the larger time span leads to larger errors, the prediction of landslide displacement based on GPS data may result in a remarkable deviation between the prediction and actual results (Qin et al. 2001). The deep displacement, if recorded in real-time, can help understand the stability condition of landslide and the development law of sliding surface more directly and effectively (Corominas et al. 2000; Stark and Choi 2008).

In this paper, 300 deep displacement data were recorded during the period of 2016.1–2017.9 by the in-place inclinometers with fiber

Bragg grating (FBG) sensors. The cumulative displacement is processed by using a time series method. Through identifying the optimal influence factors with grey correlation analysis and the SPA method, the support vector machine optimized by particle swarm optimization (SPA-PSO-SVM) prediction model is established. The validation and efficiency of the proposed prediction model have been verified against the measured displacement. The proposed model, which can realize short-term prediction of landslide accurately, has great potential to be used for landslide early warning.

Proposed displacement prediction models

Decomposition of the displacement time series

Each observed value in time series is the comprehensive result of simultaneous action of multiple factors. According to the principle of time series method, the cumulative displacement of Majiagou landslide can be divided into two parts: the trend displacement and the periodic displacement (Du et al. 2013). Consequently, the cumulative displacement can be expressed as:

$$st = ut + vt \quad (1)$$

where s_t is the cumulative displacement of a landslide, μ_t is the trend displacement, and v_t is the periodic displacement. By superimposing the prediction results of trend and periodic displacements, the cumulative landslide displacement can be obtained.

Set pair analysis

Set pair analysis was first proposed by Zhao (1989). It is a statistical theory of identical and contrary quantitative analysis on "deterministic-uncertain problems." The essence of this theory is to treat the deterministic-uncertain problem as a deterministic-uncertain system. The basic principle is to form a set pair by putting together two interrelated sets A and B. The characteristics of the two sets are analyzed, including identical relation, discrepant relation, and contrary relation (Wang et al. 2017). The connection the degree is introduced to describe the characteristic of the two interrelated sets:

$$\mu = \frac{S}{N} + \frac{P}{N}i + \frac{E}{N}j \quad (2)$$

where μ is the connection degree of set A and set B. S is the number of identical characteristics, P is the number of discrepant characteristics, and E is the number of contrary characteristics. N is the total number of characteristics of the set pair. S/N (defined as a), P/N (defined as b), and E/N (defined as c) are the identity degree, discrepancy degree, and contrary degree of set A and set B, respectively. $a, b, c \in [0, 1]$, and $a + b + c = 1$. i is the discrepancy coefficient, whose value interval is $[-1, 1]$, and j is the diagonality coefficient, which is generally set as -1 . a and cj are relatively deterministic terms; bi is relative uncertainty term.

Based on the set pair analysis method, the lag time of landslide deformation can be quantitatively determined by analyzing the dynamics correlation of periodic terms of landslide displacement and the influencing factors.

SVM and PSO algorithm

SVM algorithm

The concept of support vector machine (SVM) was first introduced by Corinna et al. (Corinna and Vapnik 1995), which shows great advantages in the fields of prediction and comprehensive evaluation. SVM regression prediction the model usually divides the sample data into the training set and the test set, and maps the training data into high latitude space, in which the linear regression is carried out (Vapnik 2000). In this way, the linear regression in high-dimensional space can be achieved so as to realize the non-linear regression and obtain the optimal decision model. The regression estimation function for SVM is:

$$f(x) = w^T \phi(x) + b \quad (3)$$

where $f(x)$ is a non-linear mapping function, w^T is the weight vector, $\phi(x)$ is non-linear mapping from the input space to the output space, and b is bias. The values of w^T and b can be obtained by using the following minimization equation:

$$D(f) = \frac{1}{2} \|W\|^2 + \frac{C}{n} \sum_{j=1}^n R_\varepsilon [y_j, f(x_j)] \quad (4)$$

where $D(f)$ is generalized optimal classification surface function considering least misclassified samples and maximum classification interval, $\|W\|^2$ is model complexity, C is penalty factor, and R is insensitive loss function (the error control function). Therefore, the optimization problem can be expressed as:

$$\left. \begin{aligned} \min Q(W, \xi) = & \frac{1}{2} \|W\|^2 + C \sum_{j=1}^n \xi_j + C \sum_{j=1}^n \xi_j^* \\ & W^T \phi(x_j) + b - y_j \leq \varepsilon + \xi_j \\ & y_j - W^T \phi(x_j) - b \leq \varepsilon + \xi_j^* \\ & \xi_j \geq 0, \xi_j^* \geq 0 (j = 1, 2, \dots, n) \end{aligned} \right\} \quad (5)$$

where ξ_j and ξ_j^* are relaxation factors.

Based on Wolf duality theory and Lagrange equation, the partial derivatives of W , a , b , ξ_j , and ξ_j^* are set as 0. The dual optimization formula is expressed in:

$$\left. \begin{aligned} L(W, a, b, \varepsilon, y) = & \min \frac{1}{2} \sum_{r,j=1}^n (a_r - a_r^*)^T H_{r,j} \cdot \\ & a, a^* \\ & (a_r - a_r^*) + \sum_{r=1}^n (a_r - a_r^*) + \sum_{r=1}^n y_r (a_r - a_r^*) \\ & \sum_{r=1}^n (a_r - a_r^*) \circ (0 \leq a_r, a_r^* \leq C) \\ & H_{r,j} = K(x_r, x_j) = \phi(x_r)^T \phi(x_j) (r = 1, 2, \dots, n) \end{aligned} \right\} \quad (6)$$

where $K(x_r, x_j)$ is the kernel function. The SVM regression prediction model can be obtained by quadratic programming:

$$f(x) = \sum_{j=1}^n (a_j - a_j^*) K(x_j, x) + b \quad (7)$$

Among the four kinds of kernel functions (e.g., linear kernel, polynomial kernel, sigmoid, and radial basis kernel function

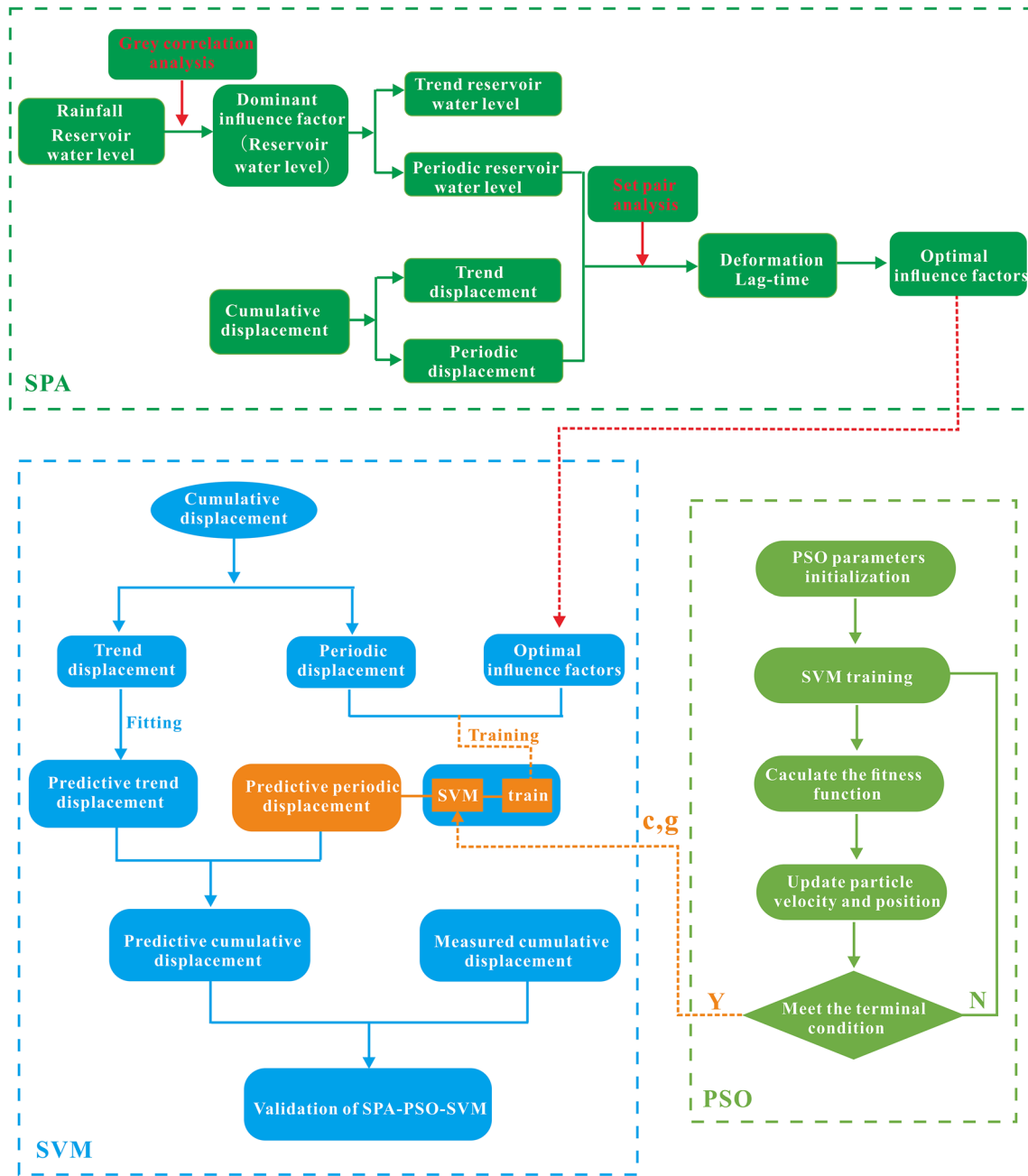


Fig. 1 Analysis flowchart of the proposed model. a Set pair analysis. b SVM prediction model. c PSO optimization model

(RBF)); the last one is the widely used. Therefore, the RBF is adopted for SVM prediction in this paper (Farzan et al. 2015).

PSO algorithm

Particle swarm optimization (PSO), which is used for solving the optimization problems, is a new evolutionary algorithm developed in recent years (Poli et al. 2007; Parsopoulos and Vrahatis 2002). Each potential solution to the problem was treated as a particle. A swarm of particles was initialized randomly to explore a problem’s search-space with the goal of finding the global optimum solution simultaneously. After finding the local and globally optimal

solutions, the particle would update its speed and new position according to certain mathematical formulae. Since the performance of the SVM model was greatly affected by the penalty factor C and the kernel function parameter g (Huang and Dun 2008), the PSO algorithm was used to optimize such parameters.

Modeling procedure

The modeling procedure of the SPA-PSO-SVM model is depicted in the flowchart as shown in Fig. 1. Firstly, the main influencing factors of landslide displacement were identified by grey correlation analysis. Then, the time series method was

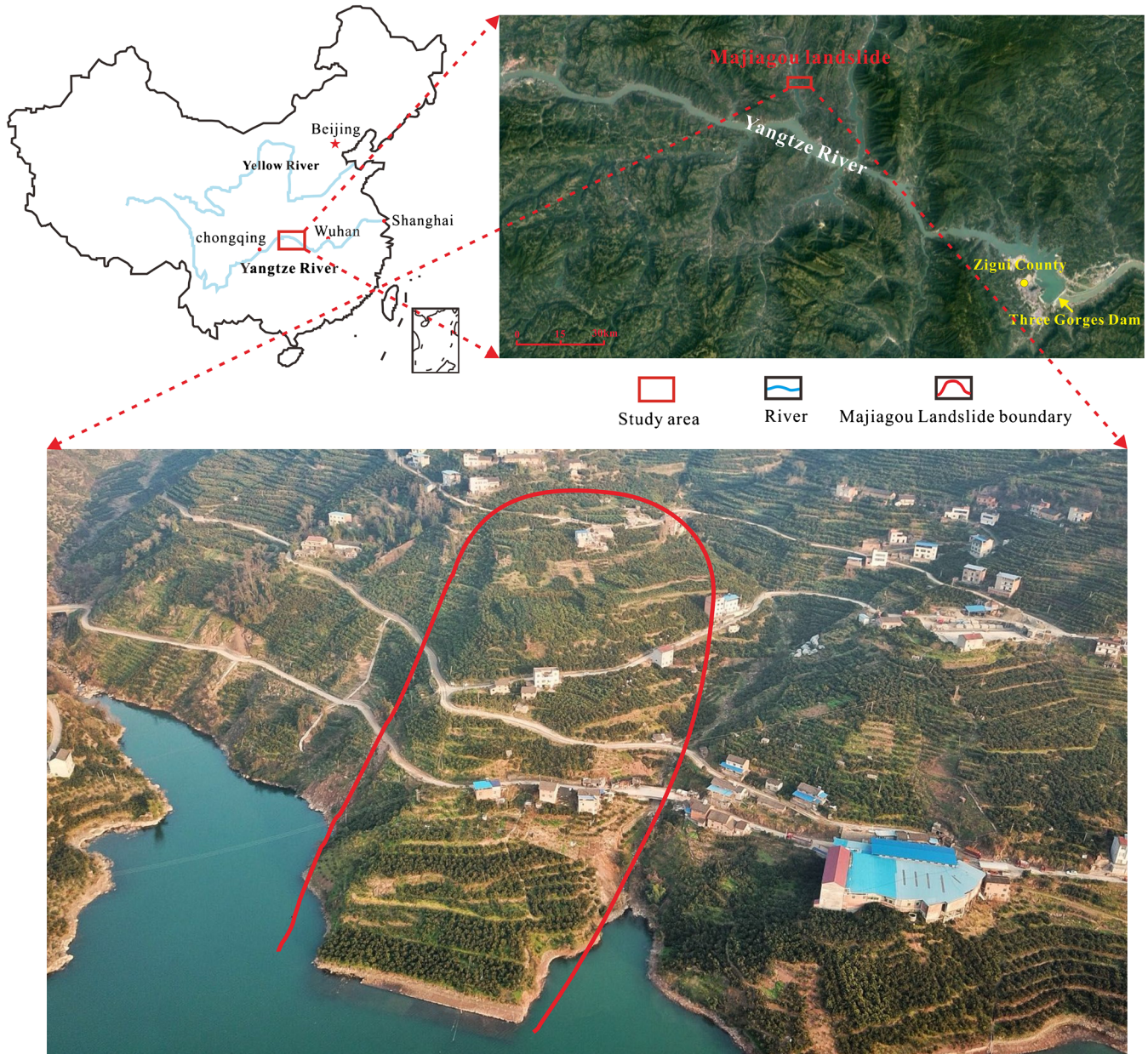


Fig. 2 Location and photograph of Majiagou landslide

adopted to decompose the cumulative displacement and dominant influence factors (Reservoir water level) into trend term and periodic term. And then, the lag time as well as the optimal influence factors was determined by set pair analysis. Then, the optimal influence factors were input into the PSO-SVM model to predict the periodic displacement. Finally, the predicted and measured displacement result were compared and analyzed for the validation of the proposed prediction model.

Case studies: Majiagou landslide

Landform

The Majiagou landslide was initiated when the reservoir was first impounded in 2003. It is 560 m long and 180–210 m wide

with an area of $9.8 \times 10^4 \text{ m}^2$. It is situated on the left bank of the Zhaxi River, a tributary river of the Yangtze River in Zigui County, Hubei Province, China (Fig. 2) (Ma et al. 2017). The Majiagou landslide is ligulate-shaped, whose gradient ranges from 12° to 20° according to the relief elevation of the ground surface. As shown in Fig. 3, the sliding orientation of the landslide is about 290° , approximately perpendicular to Zhaxi River (Zhang et al. 2018a, b). The front of the landslide is a fluvial alluvial terrace and forms a multi-stage gentle platform and steep-sided ridges. Gullies are shaped due to the long-term erosion of reservoir water on the south and north side of the slope. The elevation of the rear edge of the landslide is 285 m, and the reservoir water level fluctuates from 145 to 175 m.

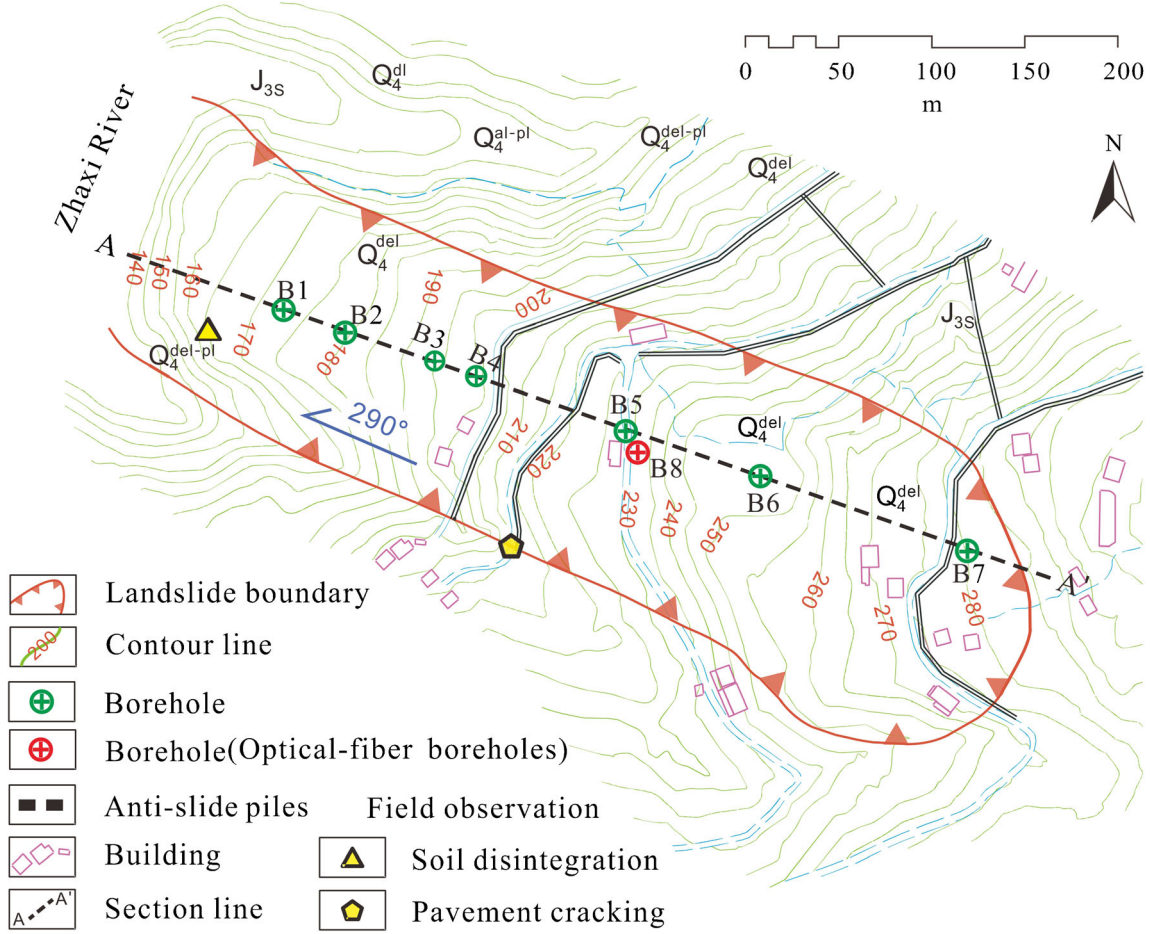


Fig. 3 Map of surveys of Majiagou landslide with the location of the monitoring network (modified from Zhang et al. 2018a, b)

Stratigraphic lithology

The Majiagou landslide mainly consists of surficial deposits and sedimentary bedrock (Fig. 4). Between them, the soft stratum,

corresponding to 18–19 m, exists. The surficial deposits, with high permeability (6.4×10^{-4} to 5.0×10^{-4} m/s), are mainly composed of residual silty clay and gravel clasts. The sedimentary bedrock,

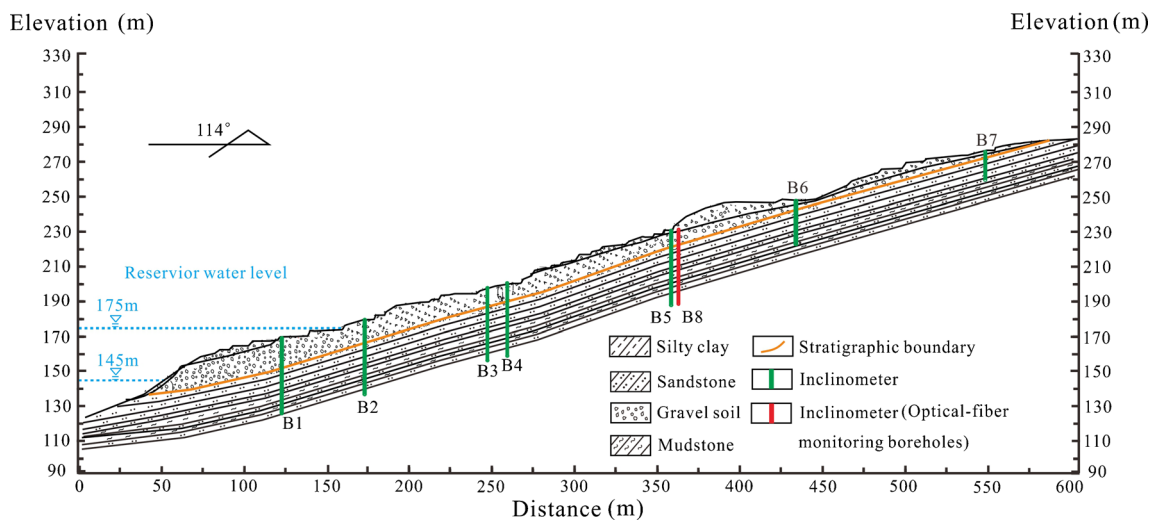


Fig. 4 Vertical profile of Majiagou landslide

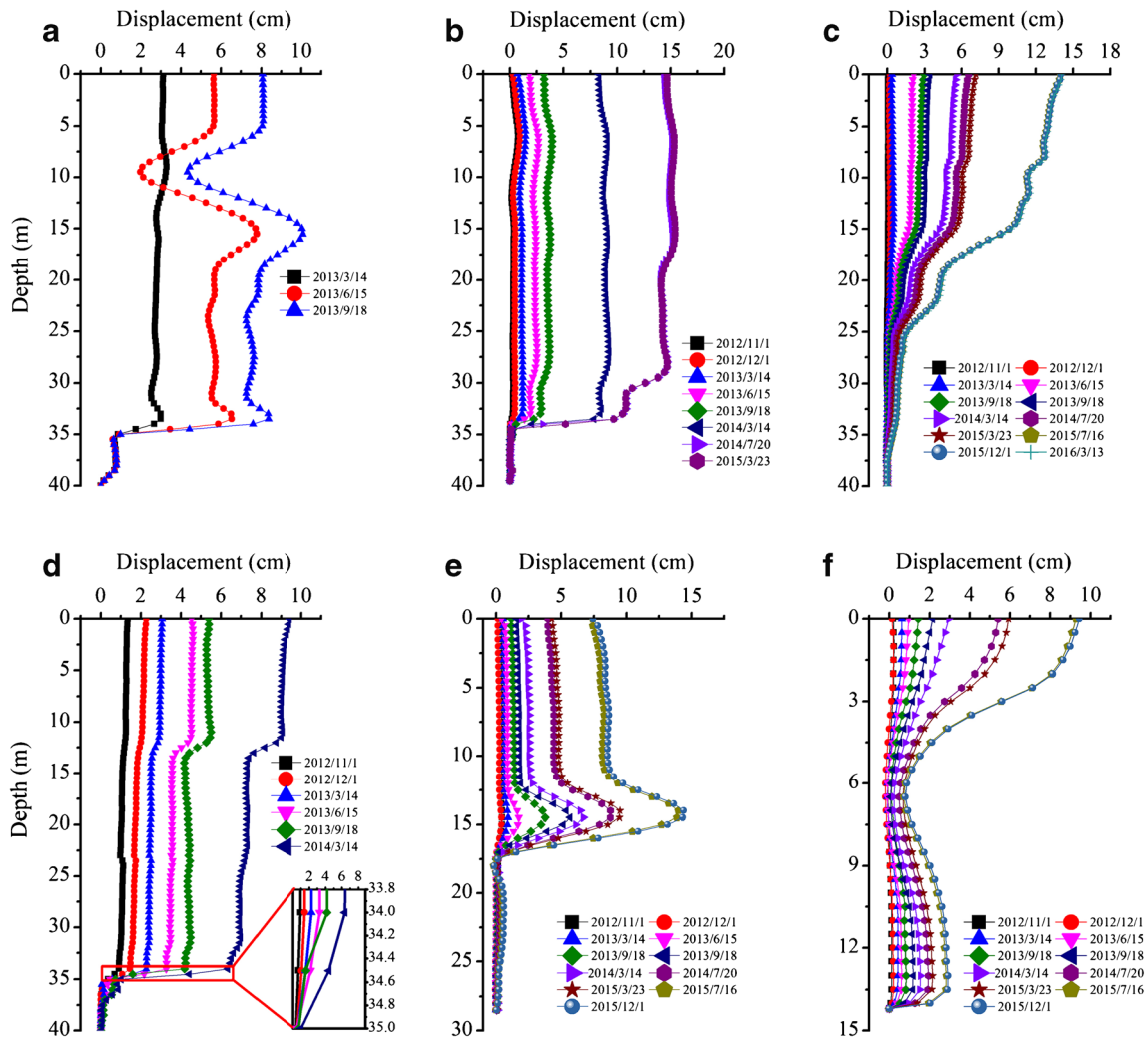


Fig. 5 Displacements measured by the inclinometers. **a** B1 inclinometer. **b** B2 inclinometer. **c** B3 inclinometer. **d** B5 inclinometer. **e** B6 inclinometer. **f** B7 inclinometer

with low permeability (1.3×10^{-7} to 6.0×10^{-6} m/s) are constituted of grey-white feldspar quartz sandstone and fine sandstone with purple-red thin silty mudstone interbedded. The silty mudstone ($\rho = 2.59 \times 10^3$ kg/m³, $\phi = 30.3^\circ$, $c = 2.99$ MPa) which is easy to be softened and highly fractured, is one of the most common strata

prone to sliding in the TGR. The physical and mechanical parameters were identified by direct shear and uniaxial compression tests (Ma et al. 2017; Zhang et al. 2018a, b). The rainfall and fluctuation of reservoir water level in TGR show apparent periodical characteristics. Rainfall is concentrated from May to

Table 1 The information of all the boreholes

Number	Elevation (m)	Depth (m)	Inclinometer type	Monitoring information	Monitoring period
B1	170	40	Conventional	Entire displacement of the inclinometer	2013.3–2013.9
B2	177	38	Conventional	Entire displacement of the inclinometer	2012.11–2015.3
B3	196	42	Conventional	Entire displacement of the inclinometer	2012.11–2016.3
B4	197	37.2	Conventional	Entire displacement of the inclinometer	2012.11–2016.3
B5	225	42	Conventional	Entire displacement of the inclinometer	2012.11–2014.3
B6	248	28.3	Conventional	Entire displacement of the inclinometer	2012.11–2015.12
B7	274	14.2	Conventional	Entire displacement of the inclinometer	2012.11–2015.12
B8	225	41	Comprehensive	Displacement of deep sliding shear zone	2016.1–2017.9 (Real time)

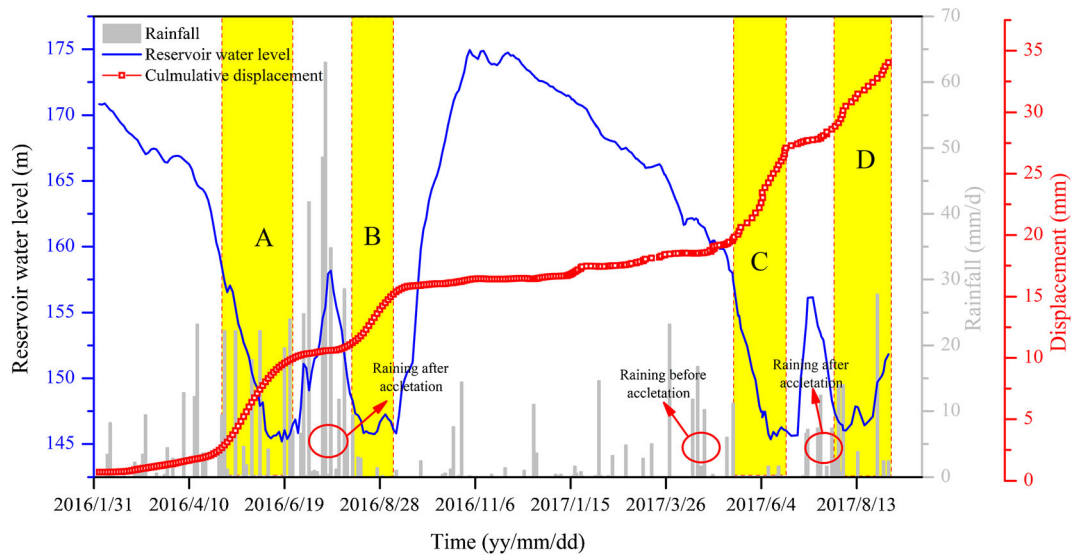


Fig. 6 The relationship between rainfall, reservoir water level and cumulative displacement monitored of Majiagou landslide

September, and the reservoir water level fluctuates between 145 and 175 m each year.

Monitoring scheme

In order to monitor further deformation and evaluate the stability of the landslide, seven inclinometers B1–B7 were installed along the main sliding direction of the landslide in November 2012 (Figs. 3 and 4). Rainfall data, transmitted to the monitoring center through the GPRS network, were collected in real-time by the weather station installed in the middle area of Majiagou landslide. The daily reservoir water level could be acquired on the website (<http://www.cjsyw.com>) released by the Hydrology Bureau of Changjiang Water Resources Commission.

The deep displacement of Majiagou landslide is obtained through the buried inclinometers and shown in Fig. 5. Based on previous research (Sun et al. 2014), there are two sliding surfaces existed in Majiagou landslide, among which, the upper one located around 19 m corresponds to the contact surface between surficial deposits and sedimentary bedrock. The deeper one located around 35 m corresponds to the weak silty mudstone interbedded in sedimentary bedrock. The deeper sliding surface is the main sliding zone (Sun et al. 2014; Zhang et al. 2018a, b), whose deformation accounts for nearly 80% of the total deformation (Fig. 5). If the instability of Majiagou landslide is induced, it will slide along the deep sliding surface. So, it is particularly important to monitor the displacement of the deep sliding zone. Therefore, in September

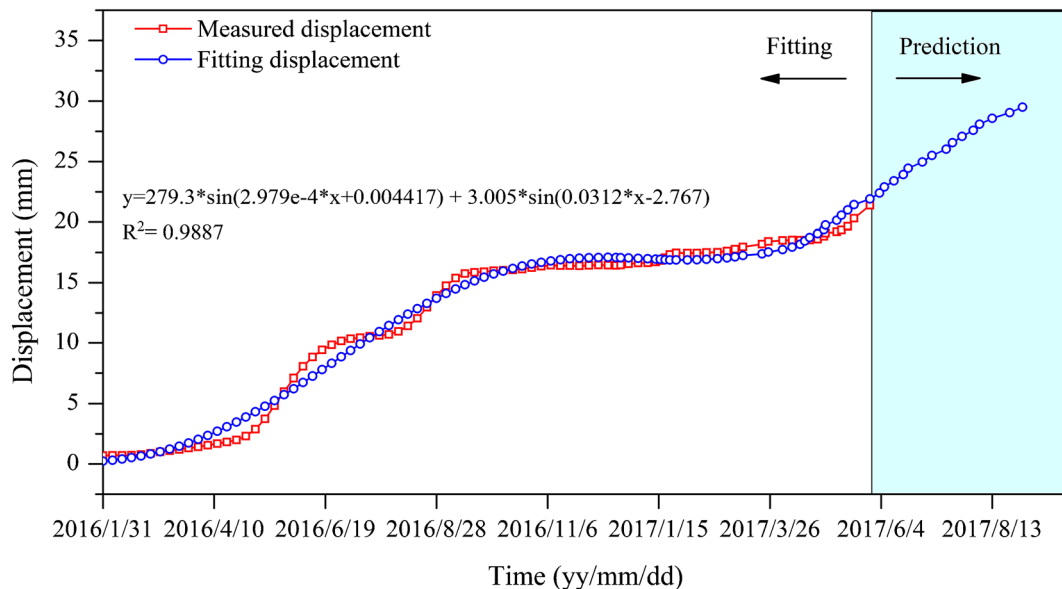


Fig. 7 Extraction of trend displacement

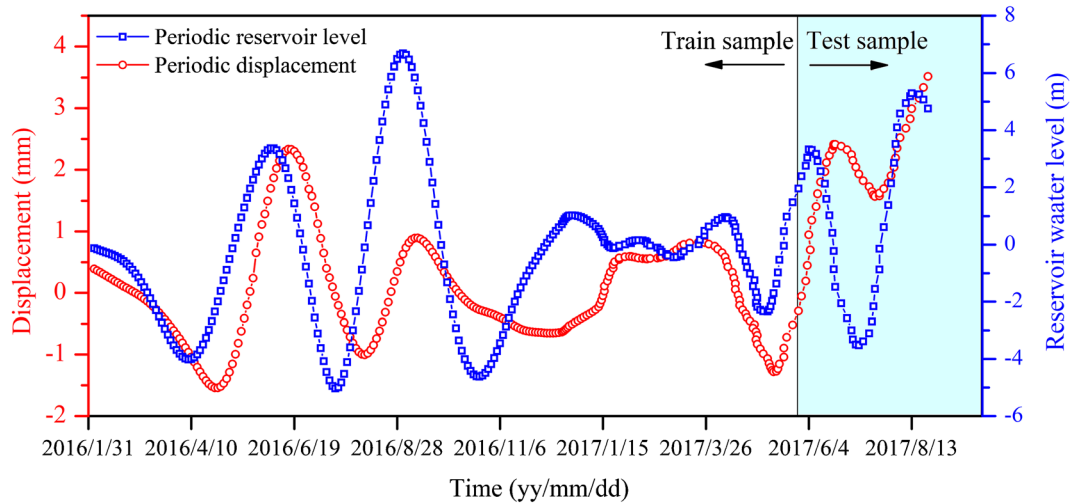


Fig. 8 Curve of periodic displacement and periodic reservoir water level

2015, a new inclinometer hole B8 was drilled next to inclinometer B5. The local enlarged displacement monitoring result of inclinometer B5 is shown in Fig. 5, which implies that the deep shear zone of landslide ranges from 34 to 35 m. Based on this, two fixed FBG-based inclinometers (whose working principle is described by Han et al. (2019)) were installed right above the bottom surface of the deeper sliding zone in inclinometer hole B8. The fixed inclinometer was connected in series with a 3-mm-diameter wire rope. The length of each in-place inclinometer is 38 cm, and the length of the wire between the in-place inclinometers is 24 cm. The deformation of the entire deep shear sliding zone can be therefore recorded in real-time. It is worth noting that the lower inclinometer is fixed with screws in case of slippage. The detail information of all the inclinometer holes is shown in Table 1.

Monitoring result and analysis

Figure 6 depicts the relationship between horizontal cumulative displacement recorded in B8 inclinometer and the hydrological factors. The cumulative horizontal displacement did not increase linearly but showed a stepped increase tendency. In early July 2016 and in March and July 2017 (the red elliptical area), intense rainfall occurred; however, the landslide displacement did not vary significantly. Whereas the concentrated rainfall accelerated the deformation of the landslide in May 2016. This indicated that rainfall was not the main controlling factor and it had little influence on the deformation of the landslide. Nevertheless, the fluctuation of reservoir water level indicated a strong seasonal influence on the deformation of Majiagou landslide. When the reservoir water level decreased rapidly (as area

A and C marked in Fig. 6), the displacement of landslide increased obviously. Due to the hydraulic gradient and the lag fluctuation of the water level in a landslide, the transient seepage occurred. Meanwhile, the transient flow inside slope deposits formed seepage force downslope along the slip direction, thereby accelerating the deformation of the landslide. When the reservoir water level rose or at a high water level, the landslide remained stable, which could be attributed to the seepage force induced by the hydraulic gradient and the effect of hydrostatic pressure (Tang et al. 2019). It was noteworthy although the water level was relatively stable, the displacement varied significantly (as area B and D marked in Fig. 6). This could be interpreted as the deformation hysteresis effect.

Furthermore, the correlation between the water level fluctuation velocity, water level, and displacement velocity are illustrated in the appendix. When the reservoir water level is lower than 150 m, the water level plays domain role in controlling the landslide displacement. No matter how the reservoir water level fluctuates, the overall deformation of Majiagou landslide is relative large. When the water level fluctuates between 150 and 160 m, the fluctuation velocity becomes the critical factor that influences the landslide displacement. When fluctuation velocity is greater than 0.4 m/day, the deformation of Majiagou landslide is not significant, whereas when fluctuation velocity is less than 0.4 m/day, the deformation rate of Majiagou landslide is at a high level. When the reservoir water level is higher than 160 m, reservoir water level plays a domain role again. The Majiagou landslide remains at a stable state. It can be inferred that the deformation characteristics are believed to be closely related to pore pressure and seepage

Table 2 The criterion of identical-discrepant-contrary relation for periodic displacement versus periodic reservoir water level

Periodic displacement	Periodic reservoir water level	
	Fall	Rise
Decrease	Contrary	Identical
Stable	Discrepant	Discrepant
Increase	Identical	Discrepant

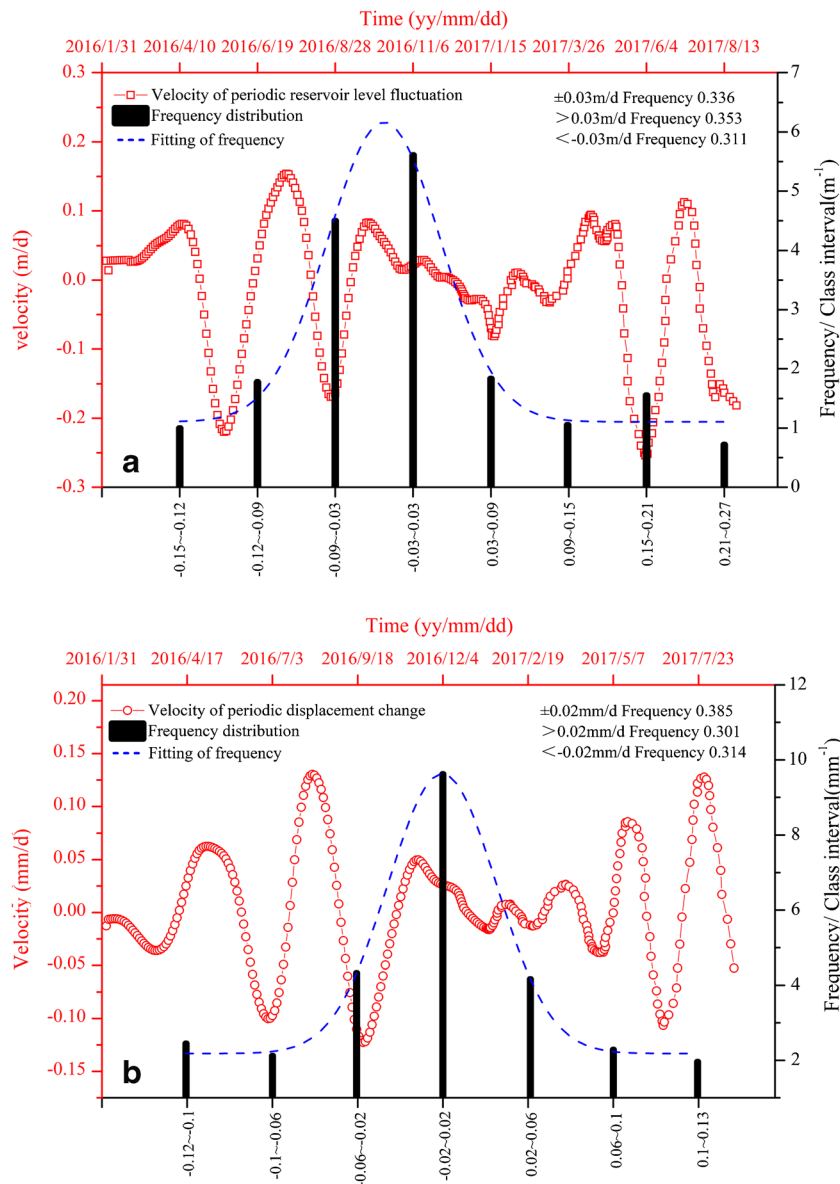


Fig. 9 a Frequency distribution of velocity of periodic reservoir water level fluctuation. b Frequency distribution of velocity of periodic displacement fluctuation

force; we will carry out in-depth analysis on the kinematic evolution of Majiagou landslide in the near future.

Deep displacement prediction of Majiagou landslide

In this paper, the deep displacement result of B8 inclinometer are selected to establish and test the prediction model, among which the first 250 is set as the calibration set and the last 50 is set as test set.

Prediction of trend displacement

In the previous landslide displacement prediction, most of the monitoring period can last 5–10 years, while the monitoring interval was usually 1 month (Shihabudheen et al. 2017; Bernardie et al. 2015). That is, limited monitoring data are distributed over a long

time span. Therefore, moving average method (Lian et al. 2014), EMD method (Xu and Niu 2018), and the polynomial method were often used to extract a relatively smooth curve as the trend displacement. However, the minimum time an interval of the Majiagou landslide displacement data was 2 days, and the time span was close to 2 years. This signified that the displacement curve varied significantly. The methods mentioned above for extracting a relatively smooth curve were not suitable. According to the characteristics of the data, by comparing the fitting effect, the triangular function was selected to fit the curve with the highest accuracy. The fitting function was:

$$y = 279.3 * \sin(2.979e^{-4} * x + 0.004417) + 3.005 * \sin(0.0312 * x - 2.767) \quad (8)$$

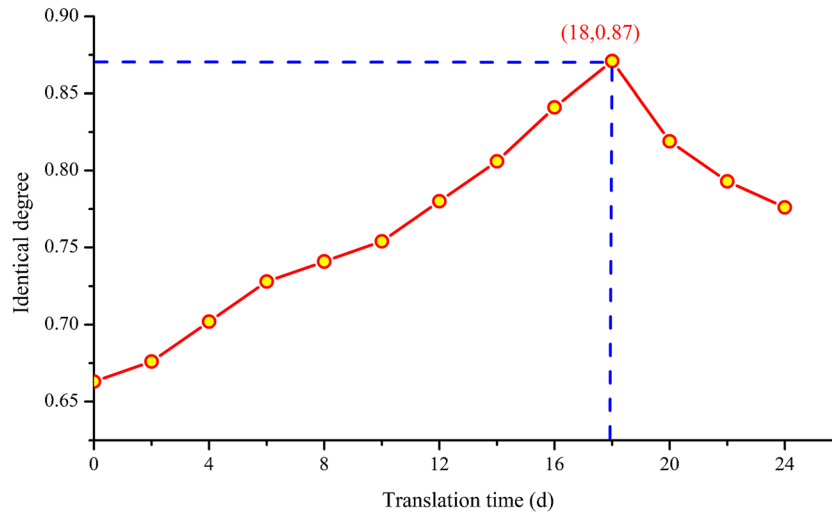


Fig. 10 Identical degree versus translation days

where y is the cumulative displacement and x is time. The R^2 and root mean square error (RMSE) of the function are 0.9887 and 0.9885, respectively.

The predicted trend displacement, acquired by using triangular fitting function, is illustrated in Fig. 7.

Prediction of periodic displacement

Extraction of periodic displacement

According to the principle of time series summation, the periodic displacement can be obtained by subtracting the trend displacement from the cumulative displacement. The periodic displacement, with obvious periodicity, is shown in Fig. 8.

The grey correlation analysis (Deng 1988), whose resolution coefficient was set as 0.5, was used to analyze the correlation between displacement with external factors. When the correlation coefficient exceeds 0.6, it can be concluded that the influencing factors are closely related to the periodic displacement (Wang et al. 2004b). The correlation coefficient between rainfall, reservoir water level, and periodic displacement of Majiagou landslide are 0.41 and 0.84, respectively, which is consistent with the analysis results as mentioned in “Monitoring result and analysis” section. It can be inferred that the deeper sliding zone is located in the weak interlayer of the sedimentary bedrock. Due to the low permeability coefficient of the bedrock, rainfall can hardly infiltrate into the weak interlayer to influence the deformation of the deep sliding zone. Therefore, the reservoir water level is chosen as the main influence factor for the prediction of periodic displacement, whose fitting function can be expressed as:

$$y = 162.5 + 13.12 \cdot \cos(3.385e-2 \cdot x) + 0.8833 \cdot \sin(3.385e-2 \cdot x) - 1.594 \cdot \cos(6.77e-2 \cdot x) - 3.508 \cdot \sin(6.77e-2 \cdot x) \quad (9)$$

where y is the reservoir water level, and x is time. The R^2 and RMSE of the function are 0.9295 and 1.563, respectively. Similarly, based on the principle of time series summation, the periodic reservoir water level can be obtained as shown in Fig. 8.

Deformation lag time

Before identifying the lag time, the threshold Q_1 (m/day) of periodic water level fluctuation and the threshold Q_2 (mm/day) of periodic displacement change were introduced. The fluctuation of periodic water level can be divided into three states: stable stage, rising stage, and falling stage according to the three criteria of “within the fluctuation Q_1 ,” “rising over Q_1 ,” and “falling over Q_1 .” Similarly, the variation of periodic displacement can also be divided into three states: stable stage, decrease stage, and increase stage according to the three criteria of “within the variation Q_2 ,” “increasing over Q_2 ,” and “decreasing over Q_2 .” The identical, discrepant, and contrary relations between periodic displacement and periodic reservoir water level are established, as listed in Table 2. In view of the above, determining the values of Q_1 and Q_2 become a key point. The threshold value should try to make the number of three states of the two sets relatively balanced, that is, each state is at the same significant level so as to avoid making the number of one state is significantly larger than the other two states. If so, the respond of the set pair to each translation would become remarkable (Liu et al. 2009). The threshold can be effectively determined by examining the frequency distribution of the velocity of periodic water level fluctuation and velocity of periodic displacement change. As shown in Fig. 9a, according to the fluctuation velocity (ranges from $-0.15 \sim 0.27$ m/day) of the periodic water level (as marked with a red square), the frequency distribution of the fluctuation velocity of the periodic reservoir water level can be obtained. When $Q_1 = 0.03$ m/day, the frequency of velocity of reservoir level fluctuation within (± 0.03 m/day) was 0.336, and the frequency below -0.03 m/day and above 0.03 m/day were 0.311 and 0.353, respectively. It signifies that the number of three states of periodic water level is almost the same and they are at the same significant level. Consequently, $Q_1 = 0.03$ m/day was chosen as the key value. Similarly, as shown in Fig. 9b, the frequency of velocity of periodic displacement change varies within (± 0.02 mm/day) was 0.385. While the variation velocity was greater than 0.02 mm/day and less than -0.02 mm/day, the frequencies were 0.301 and 0.314,

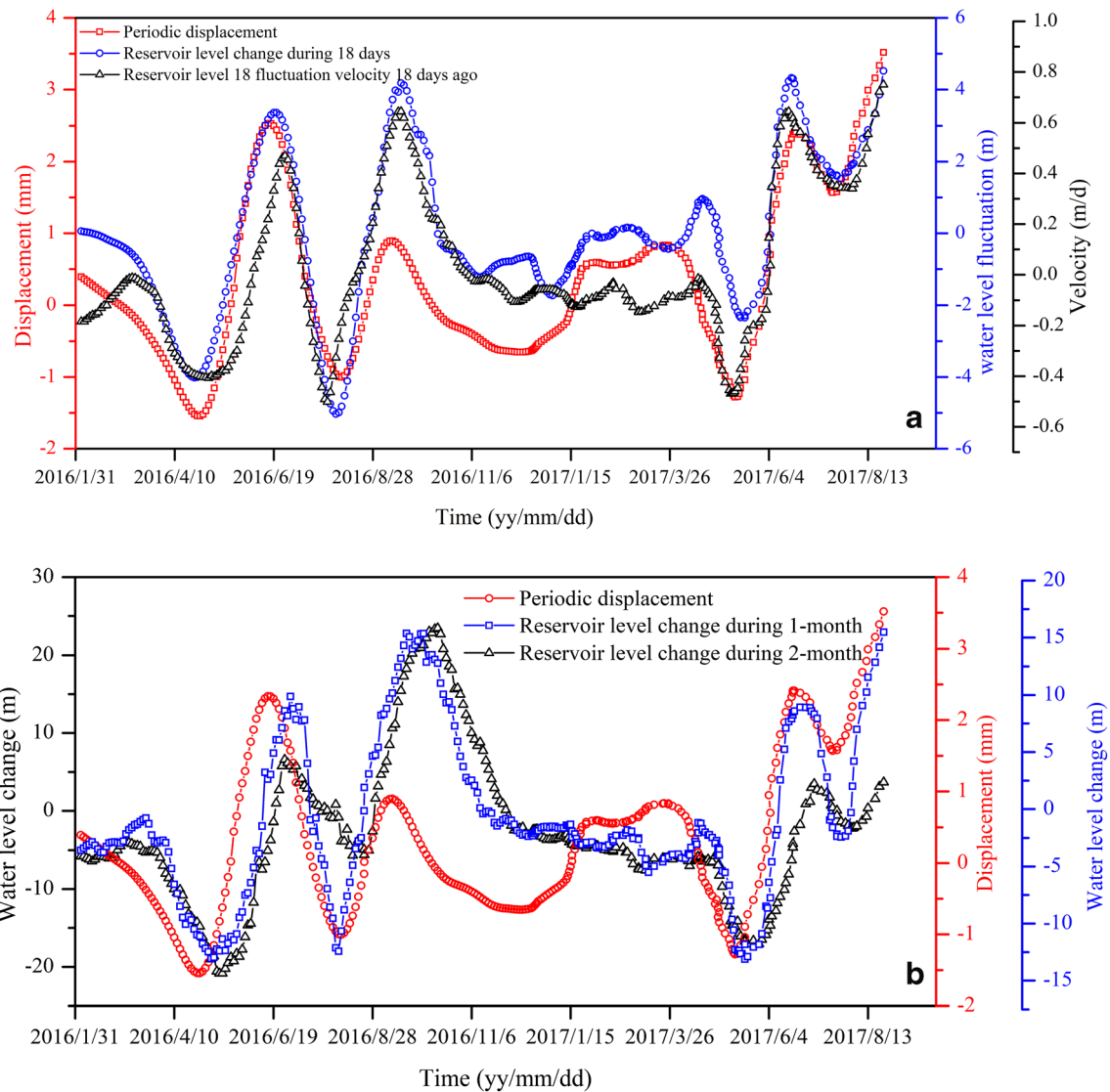


Fig. 11 Correlation between the periodic displacement and fluctuation of reservoir water level. **a** The optimal influence factors of reservoir water level determined by SPA method. **b** The influence factors of reservoir water level selected on experience

respectively. Therefore, the periodic displacement variation threshold Q_2 was determined as 0.02 mm/day.

As the larger the value of an identical degree, the better the correlation between the two sequences is. In order to quantitatively identify the lag time, the periodic term of reservoir water level was translated with a step of 2 days continuously. As shown in Fig. 10, the maximum of the identical degree between the periodic terms of reservoir water level and displacement can be reached when the translation time was 18 days.

According to the lag time, the reservoir level change during 18 days and the reservoir water level fluctuation velocity 18 days ago were selected as the optimal factors. For comparison, the reservoir water level change during 1 and 2 months was selected as input factors (Zhou et al. 2016). The variation of influence factors determined by the SPA method exhibited good agreement with the periodic displacement (Fig. 11a). While the time series curve of

the empirically selected factors lagged slightly behind that of periodic displacement (Fig. 11b).

The cumulative displacement could not only reflect the general trend of landslide deformation, but it also reflected the variation characteristics of periodic displacement (Miao et al. 2018). The accurate prediction of landslide deformation could hardly attain by only considering the triggers factors and ignoring the evolutionary state of the landslide. Therefore, the displacement change during 18 days and the displacement velocity 18 days ago were chosen as the optimal influence factors. Similarly, the displacement change during 1 and 2 months was selected as the input factor (Zhou et al. 2016). As shown in Fig. 12a, the displacement change during 18 days and the displacement velocity 18 days ago correspond to the peak and trough positions of the periodic displacement. Beyond that, the overall variation trend is also consistent. By contrast, as shown in Fig. 12b, the hysteresis

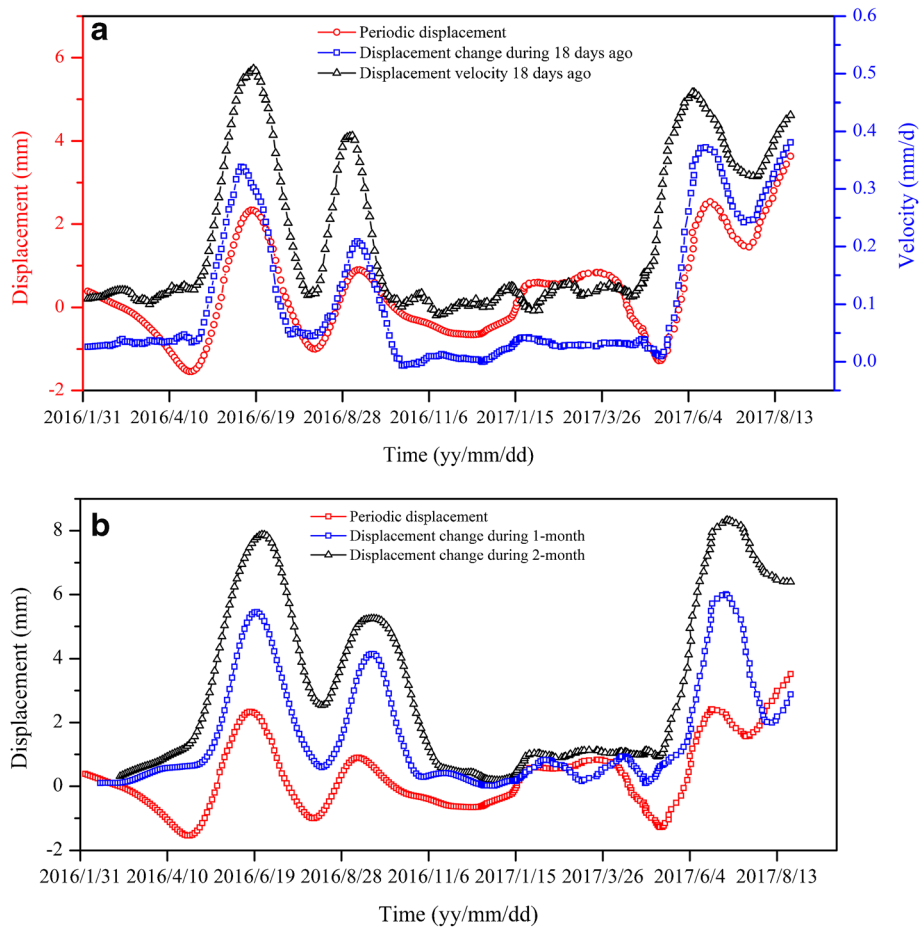


Fig. 12 Correlation between the periodic displacement and cumulative displacement change. **a** The optimal influence factors of displacement determined by SPA method. **b** The influence factors of displacement selected on experience

phenomenon also exists between the curve of displacement change during 1 and 2 months and periodic displacement.

In summary, the reservoir level change during 18 days and reservoir water level fluctuation velocity 18 days ago as well as the displacement change during 18 days and the displacement

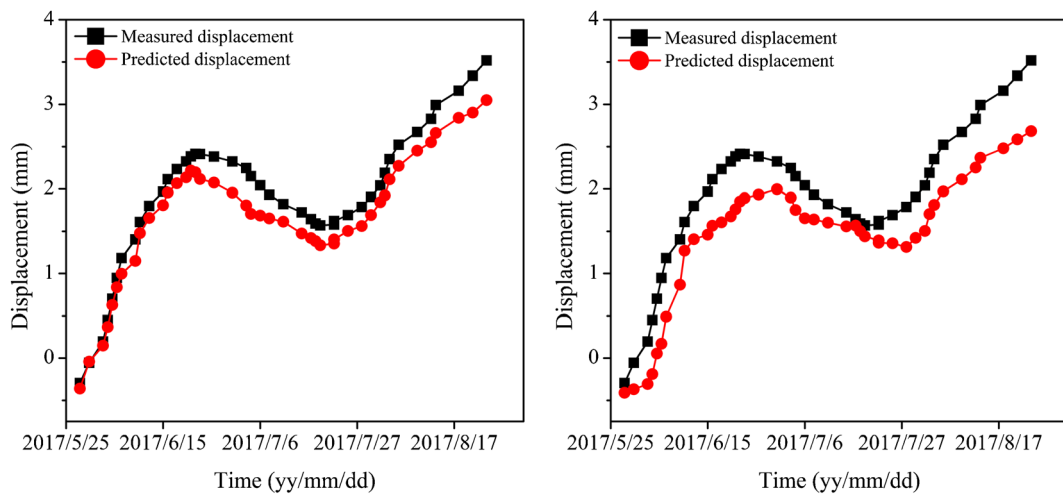


Fig. 13 Comparisons of predicted and measured periodic displacements. **a** The predicted displacement obtained by SPA-PSO-SVM model. **b** The predicted displacement obtained by PSO-SVM model

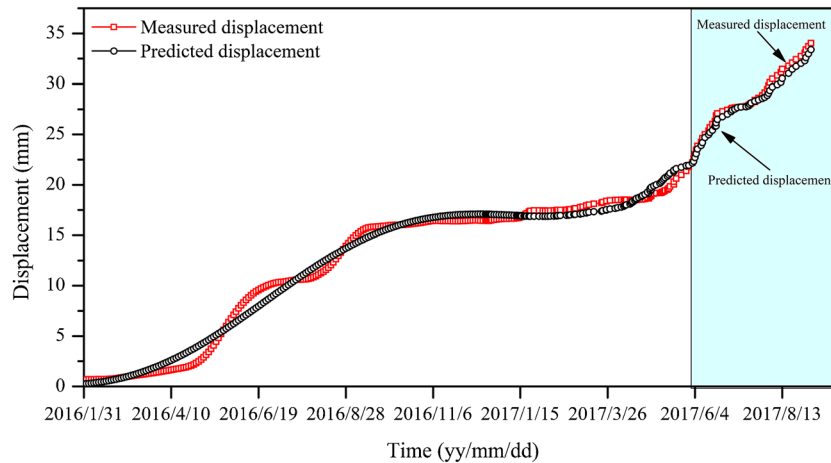


Fig. 14 Comparison of the predicted and measured cumulative displacement

velocity 18 days ago were chosen as the optimal influence factors of the SPA-PSO-SVM model.

Periodic displacement prediction

The libsvm toolbox (Chang and Lin 2011), whose parameters were optimized by PSO, was used to predict the periodic displacement. After 200 times iterations, the optimal penalty factors C and kernel function parameters g for the SPA-PSO-SVM model are 3.7132 and 0.5223. For PSO-SVM model, they are 11.2372 and 3.9796, respectively. After running the PSO-SVM prediction model with the optimal and empirical selected influencing factors, the predicted periodic displacement can be obtained (see Fig. 13). Figure 13a shows the predicted result based on the SPA-PSO-SVM model, which signifies that the periodic displacement is well predicted with the proposed model. The results of the predicted periodic displacement based on PSO-SVM model, as shown in Fig. 13b, lag behind the measured values and exhibits a larger deviation compared with the measured data. Comparing with the measured result, it is found that the RMSE and the mean absolute percentage error (MAPE) of SPA-PSO-SVM model are 0.28 and 12.8, respectively, which is significantly smaller than that of PSO-SVM model with the RMSE of 0.53 and the MAPE of 29.7, supporting the assertion that prediction accuracy was obviously improved by using this proposed model.

Cumulative displacement prediction

As shown in Fig. 14, the cumulative prediction displacement could be obtained by summing the fluctuating displacement and the trend displacement. The predicted cumulative displacement, with the correlation coefficient of 0.99 and the RMSE of 0.33, is in good agreement with that of measured. Consequently, the proposed model is feasible in the landslide displacement prediction.

Discussions

Rainfall infiltration and reservoir water level fluctuation can cause soil water changes, affect the stress state, induce dynamic and static water pressure, reduce shear strength of soil, and thus influence the evolution of the landslide (Paronuzzi et al. 2013; Hu et al. 2017), which are regarded as the major triggering factors of

landslide deformation (Lepore et al. 2012; Bui et al. 2017). However, in this study, rainfall could hardly infiltrate into the weak inter-layer to affect the evolution process of the deep sliding zone. While deploying machine learning method to make prediction, it was not the more influence factors input, the better prediction results would be. If the input influence factor is weak related to the output displacement, on the contrary, will reduce the prediction accuracy (Deng et al. 2017). Through grey correlation analysis, by removing the rainfall factors, the fluctuation of reservoir water level was selected as the main influencing factors.

SVM is a small sample learning method based on statistical learning theory, which has good generalization performance by using the structural risk minimization principle. It overcomes the limitations of local optimum, over-fitting, and slow convergence speed existed in a mathematical method and traditional neural network. The SVM model based on the particle PSO algorithm has been applied in landslide prediction (Wu et al. 2016; Chawla et al. 2018). However, current research is mostly in the qualitative description stage; how to quantitatively characterize the lag effect and select the most relevant influencing factors has been a thorny problem for a long time.

Aiming at filling this gap, SPA method was adopted to analyze the dynamic relationship between periodic displacement and influencing factors. After selecting the optimal influencing factors, the proposed SPA-PSO-SVM model can attain a relatively higher accuracy than that of PSO-SVM model.

Conclusions

Since the first impoundment of the Three Gorges Reservoir, more and more attention has been drawn on the deformation and instability of the reservoir slopes. Landslides usually undergo long-term deformation before failure occurs (Ren et al. 2015). Therefore, the prediction of landslide displacement has become an economical and efficient way to migrate further risk. Taking Majiagou landslide as an example, the fiber optic monitoring technology and SPA-PSO-SVM prediction model were combined to facilitate the accurate monitoring and prediction of landslide displacements. The conclusions were drawn below:

1. There are two sliding surfaces existed in Majiagou landslide. The deeper one developed in the weak interlayer of sedimentary bedrock is the main sliding zone. Due to the low permeability coefficient of bedrock, rainfall can hardly infiltrate into the weak bedrock interlayer. Consequently, the deep deformation of the landslide is mainly controlled by the fluctuation of reservoir water level while rainfall has minor influence.
2. The time series analysis method was used to decompose the displacement and reservoir water level into trend term and periodic term. By continuously translating the periodic term of these two-time series, the maximum identical degree could be determined with the SPA method. The deformation lag time of Majiagou landslide was identified to be 18 days.
3. According to the lag time, the optimal influence factors were selected and input into the SPA-PSO-SVM prediction model. The results showed that the RMSE and MAPE of the predicted displacement are 0.28 and 12.8, which is significantly smaller than the PSO-SVM model with the RMSE of 0.53 and the MAPE of 29.7.
4. The proposed SPA-PSO-SVM model provides a scientific method of selecting influence factors rather than relying on experience. This model has a guiding significance in the landslide deformation prediction study.>

This manuscript proposed hybrid machine learning method for the displacement prediction of a landslide with deformation hysteresis effect involved. If the deformation of a landslide is induced by stress (e.g., loading, excavation or earthquake) which does not involve hysteresis effect, this proposed method shows no advantages. However, for the reservoir landslide or rainfall-triggered landslide involving deformation hysteresis effect, if the monitoring time interval is greater than the lag time, the deformation lag time cannot be determined by SPA method. This method is no longer applicable. Another limitation is the machine learning method that if you do not have enough early training data, you cannot obtain a model to make prediction. Even though SVM is a small sample learning method which can achieve good prediction result with limited data, dozens or hundreds of data are still needed.

Acknowledgments

The authors gratefully acknowledge the financial support provided by the State Key Program of National Natural Science Foundation of China (Grant No. 41427801) and the National Key R & D Program of China (Grant No. 2018YFC1505104). Special thanks are given to B. P. Naveen of Amity University Haryana for making corrections to this paper in English. The authors also thank the efforts of the technicians from Suzhou NanZee Sensing Technology Co., Ltd. and other participants in this research work.

References

Akbarimehr M, Motagh M, Haghshenas-Haghighi M (2013) Slope stability assessment of the Sarcheshmeh landslide, Northeast Iran, investigated using InSAR and GPS observations. *Remote Sens* 5(8):3681–3700

Baldi P, Cenni N, Fabris M, Zanutta A (2008) Kinematics of a landslide derived from archival photogrammetry and GPS data. *Geomorphology* 102(3-4):435–444

Bernardie S, Desramaut N, Malet JP, Gourlay M, Grandjean G (2015) Prediction of changes in landslide rates induced by rainfall. *Landslides* 12(3):481–494

Bui DT, Tuan TA, Hoang ND, Thanh NQ, Nguyen DB, Van Liem N, Pradhan B (2017) Spatial prediction of rainfall-induced landslides for the Lao Cai area (Vietnam) using a hybrid intelligent approach of least squares support vector machines inference model and artificial bee colony optimization. *Landslides* 14(2):447–458

Carlà T, Intrieri E, Di Traglia F, Nolesini T, Gigli G, Casagli N (2017) Guidelines on the use of inverse velocity method as a tool for setting alarm thresholds and forecasting landslides and structure collapses. *Landslides* 14(2):517–534

Chang CC, Lin CJ (2011) LIBSVM: a library for support vector machines. *ACM Trans Intell Syst Technol* 2(3):27

Chawla A, Chawla S, Pasupuleti S, Rao ACS, Sarkar K, Dwivedi R (2018) Landslide susceptibility mapping in Darjeeling Himalayas, India. *Adv Civ Eng* 2018:6416492

Corinna C, Vapnik V (1995) Support-vector networks. *Mach Learn* 20(3):273–297

Corominas J, Moya J, Lloret A, Gili JA, Angeli MG, Pasuto A, Silvano S (2000) Measurement of landslide displacements using a wire extensometer. *Eng Geol* 55(3):149–166

Deng J (1988) Grey forecasting and decision making. Huazhong University of Science and Technology Press, Wuhan, pp 86–128

Deng DM, Liang Y, Wang LQ, Wang CS, Sun ZH, Wang C, Dong MM (2017) Displacement prediction method based on ensemble empirical mode decomposition and support vector machine regression—a case of landslides in Three Gorges Reservoir area. *Rock Soil Mech* 12(38):1001–1009

Du J, Yin K, Lacasse S (2013) Displacement prediction in colluvial landslides, three Gorges reservoir, China. *Landslides* 10(2):203–218

Farzan A, Mashohor S, Ramlil AR, Mahmud R (2015) Boosting diagnosis accuracy of Alzheimer's disease using high dimensional recognition of longitudinal brain atrophy patterns. *Behav Brain Res* 290:124–130

Han HM, Zhang L, Shi B, Wei GQ (2019) Prediction of deep displacement of Majiagou landslide based on optical fiber monitoring and PSO-SVM model. *J Eng Geol* 27(4):853–861. <https://doi.org/10.13544/j.cnki.jeg.2018-257> (in chinese)

Hu XL, Tan FL, Tang HM, Zhang GC, Su AJ, Xu C, Zhang YM, Xiong CR (2017) In-situ monitoring platform and preliminary analysis of monitoring data of Majiagou landslide with stabilizing piles. *Eng Geol* 228:323–336. <https://doi.org/10.1016/j.enggeo.2017.09.001>

Huang CL, Dun JF (2008) A distributed PSO-SVM hybrid system with feature selection and parameter optimization. *Appl Soft Comput* 8(4):1381–1391

Huang F, Huang J, Jiang S, Zhou C (2017) Landslide displacement prediction based on multivariate chaotic model and extreme learning machine. *Eng Geol* 218:173–186

Jiao YY, Zhang HQ, Tang HM, Zhang XL, Adoko AC, Tian HN (2014) Simulating the process of reservoir-impoundment-induced landslide using the extended DDA method. *Eng Geol* 182:37–48

Lepore C, Kamal SA, Shanahan P, Bras RL (2012) Rainfall-induced landslide susceptibility zonation of Puerto Rico. *Environ Earth Sci* 66(6):1667–1681

Li XZ, Xu Q (2003) Models and Criteria of Landslide Prediction. *J Catastrophol* 18(4):71–78 (in Chinese)

Lian C, Zeng Z, Yao W, Tang H (2014) Ensemble of extreme learning machine for landslide displacement prediction based on time series analysis. *Neural Comput & Applic* 24(1):99–107

Liu X, Tang HM, Liu Y (2009) Landslide deformation dynamic modeling research based on set pair analysis. *Rock Soil Mech* 30(8):166–173 (in chinese)

Ma JW, Tang HM, Liu X, Hu X, Sun M, Song Y (2017) Establishment of a deformation forecasting model for a step-like landslide based on decision tree C5.0 and two-step cluster algorithms: a case study in the Three Gorges Reservoir area, China. *Landslides* 14(3):1275–1281

Miao F, Wu Y, Xie Y, Li Y (2018) Prediction of landslide displacement with step-like behavior based on multialgorithm optimization and a support vector regression model. *Landslides* 15(3):475–488

Paronuzzi P, Rigo E, Bolla A (2013) Influence of filling–drawdown cycles of the Vajont reservoir on Mt. Toc slope stability. *Geomorphology* 191:75–93

Parsopoulos KE, Vrahatis MN (2002) Recent approaches to global optimization problems through particle swarm optimization. *Nat Comput* 1(2-3):235–306

Poli R, Kennedy J, Blackwell T (2007) Particle swarm optimization. *Swarm Intell* 1(1):33–57

Qin S, Jiao JJ, Wang SJ (2001) The predictable time scale of landslides. *B Eng Geol Environ* 59(4):307–312

Ren F, Wu X, Zhang K, Niu R (2015) Application of wavelet analysis and a particle swarm-optimized support vector machine to predict the displacement of the Shuping landslide in the Three Gorges, China. *Environ Earth Sci* 73(8):4791–4804

Shihabuddeen KV, Pillai GN, Peethambaran B (2017) Prediction of landslide displacement with controlling factors using extreme learning adaptive neuro-fuzzy inference system (ELANFIS). *Appl Soft Comput* 61:892–904

Stark TD, Choi H (2008) Slope inclinometers for landslides. *Landslides* 5(3):339–350

- Sun YJ, Zhang D, Shi B, Tong HJ, Wei GQ, Wang X (2014) Distributed acquisition, characterization and process analysis of multi-field information in slopes. *Eng Geol* 182:49–62. <https://doi.org/10.1016/j.enggeo.2014.08.025>
- Tang MG, Xu Q, Yang H, Li SL, Iqbal Javed FXL, Huang XB, Cheng WM (2019) Activity law and hydraulics mechanism of landslides with different sliding surface and permeability in the Three Gorges Reservoir Area, China. *Eng Geol* 260:105212
- Vallet A, Charlier JB, Fabbri O, Bertrand C, Carry N, Mudry J (2016) Functioning and precipitation-displacement modelling of rainfall-induced deep-seated landslides subject to creep deformation. *Landslides* 13(4):653–670
- Vapnik VN (2000) The nature of statistical learning theory. *Statistics for Engineering and Information Science*. Springer, New York
- Wang F, Li T (2009) Landslide disaster mitigation in Three Gorges reservoir, China. *Mt Res Dev* 30:184–185
- Wang FW, Zhang YM, Huo ZT, Matsumoto T, Huang BL (2004a) The July 14, 2003 Qianjiangping landslide, three gorges reservoir, China. *Landslides* 1(2):157–162
- Wang Y, Yin K, An G (2004b) Grey correlation analysis of landslide sensitive factor. *Rock Soil Mech* 01:91–93
- Wang Y, Jing H, Yu L, Su H, Luo N (2017) Set pair analysis for risk assessment of water inrush in karst tunnels. *B Eng Geol Environ* 76(3):1199–1207
- Wolter A, Stead D, Clague JJ (2014) A morphologic characterisation of the 1963 Vajont Slide, Italy, using long-range terrestrial photogrammetry. *Geomorphology* 206:147–164
- Wu X, Shen S, Niu R (2016) Landslide susceptibility prediction using GIS and PSO-SVM. *Geomatics Inf Sci Wuhan Univ*
- Xu S, Niu R (2018) Displacement prediction of Baijiabao landslide based on empirical mode decomposition and long short-term memory neural network in Three Gorges area, China. *Comput Geosci* 111:87–96
- Zhang YM, Hu XL, Tannant DD, Zhang G, Tan FL (2018a) Field monitoring and deformation characteristics of a landslide with piles in the Three Gorges Reservoir area. *Landslides* 15(3):581–592. <https://doi.org/10.1007/s10346-018-0945-9>
- Zhang CC, Zhu HH, Liu S, Shi B, Zhang D (2018b) A kinematic method for calculating shear displacements of landslides using distributed fiber optic strain measurements. *Eng Geol* 234:83–96
- Zhang W, Xiao R, Shi B, Zhu HH, Sun Y (2019) Forecasting slope deformation field using correlated grey model updated with time correction factor and background value optimization. *Eng Geol* 260:105215
- Zhao KQ (1989) Theory and analysis of set pair e a new concept and system analysis method. In: *Conference Thesis of System Theory and Regional Planning*, pp 87–91
- Zhou C, Yin K, Cao Y, Ahmed B (2016) Application of time series analysis and PSO-SVM model in predicting the Bazimen landslide in the Three Gorges Reservoir, China. *Eng Geol* 204:108–120

Electronic supplementary material The online version of this article (<https://doi.org/10.1007/s10346-020-01426-2>) contains supplementary material, which is available to authorized users.

L. Zhang · B. Shi (✉) · **H. Zhu** (✉) · **H. Han**

School of Earth Sciences and Engineering,
Nanjing University,
Nanjing, 210023, China
Email: shibin@nju.edu.cn
Email: zhh@nju.edu.cn

X. B. Yu · X. Fan

Department of Civil Engineering,
Case Western Reserve University,
Cleveland, OH 44106, USA